

Higgs Signal for $h \rightarrow aa$ at Hadron Colliders

Marcela Carena

Fermi National Accelerator Laboratory, Batavia, IL 60510, USA

E-mail: carena@fnal.gov

Tao Han and Gui-Yu Huang

Department of Physics, University of Wisconsin, Madison, WI 53706, USA

E-mail: than@hep.wisc.edu, ghuang@hep.wisc.edu

Carlos E.M. Wagner

HEP Division, Argonne National Laboratory, Argonne, IL 60439, USA

Enrico Fermi Institute and Kavli Institute for Cosmological Physics,

Physics Department, University of Chicago, Chicago, IL 60637, USA

E-mail: cwagner@hep.anl.gov

ABSTRACT: We assess the prospect of observing a neutral Higgs boson at hadron colliders in its decay to two spin-zero states, a , for a Higgs mass of 90–130 GeV, when produced in association with a W or Z boson. Such a decay is allowed in extensions of the MSSM with CP-violating interactions and in the NMSSM, and can dominate Higgs boson final states, thereby evading the LEP constraints on standard Higgs boson production. The light spin-zero state decays primarily via $a \rightarrow b\bar{b}$ and $\tau^+\tau^-$, so this signal channel retains features distinct from the main backgrounds. Our study shows that at the Tevatron, there may be potential to observe a few events in the $b\bar{b}\tau^+\tau^-$ or $b\bar{b}b\bar{b}$ channels with relatively small background, although this observation would be statistically limited. At the LHC, the background problem is more severe, but with cross sections and integrated luminosities orders of magnitude larger than at the Tevatron, the observation of a Higgs boson in this decay mode would be possible. The channel $h \rightarrow aa \rightarrow b\bar{b}b\bar{b}$ would provide a large statistical significance, with a signal-to-background ratio on the order of 1 : 2. In these searches, the main challenge would be to retain the adequate tagging efficiency of b 's and τ 's in the low p_T region.

KEYWORDS: Higgs, NMSSM, Tevatron, LHC.

Contents

1. Introduction	1
2. Signal Processes and Parameter Choices	3
2.1 Signal Processes	3
2.2 Parameter Choices	3
3. $h \rightarrow aa$ at the Tevatron	4
3.1 The $2b2\tau$ Channel	4
3.2 Signal Event Rate for the $2b2\tau$ Channel	5
3.3 Background and Cuts for the $2b2\tau$ Channel	5
3.4 The $4b$ Channel	9
4. $h \rightarrow aa$ at the LHC	11
4.1 The $2b2\tau$ Channel	12
4.2 The $4b$ Channel	13
5. Summary	15

1. Introduction

The elucidation of the mechanism leading to the origin of mass of all observed elementary particles is one of the main goals in high energy physics. The simple Standard Model (SM) picture, based on the spontaneous breakdown of the electroweak symmetry by the vacuum expectation value (vev) of an elementary Higgs field, seems to lead to a picture that is consistent with all experimental observables, provided the Higgs boson mass is smaller than about 250 GeV. Moreover, the best fit to the precision electroweak observables measured at the LEP, SLC and Tevatron experiments lead to values of the Higgs mass of the order of or smaller than the present bound coming from direct searches at LEP, $m_{H_{\text{SM}}} \gtrsim 114 \text{ GeV}$ [1].

In spite of the extraordinary good agreement of the experimental observations with the SM predictions, there are many theoretical motivations to go beyond the SM description. Several extensions of the SM exist in the literature, and in most of them the Higgs sector is extended to a more complicated structure, often including at least two Higgs doublets. The requirement of preserving the good agreement with experimental data can be easily fulfilled in extensions, like supersymmetry, in which

the effect of the additional particles on the precision electroweak observables rapidly vanish with increasing values of the new particle masses. An extension of the Higgs sector will generally require a revision of the direct and indirect limits on the Higgs mass. In particular, the direct search for Higgs bosons may be affected by additional decay modes that are beyond the ones analyzed by the LEP collaborations.

As an example, let us consider the minimal supersymmetric extension of the SM (MSSM). In the MSSM, there is an additional Higgs doublet, leading, in the absence of CP-violation in the Higgs sector, to two CP-even and one CP-odd Higgs boson states. At large values of $\tan\beta$, the ratio of the two Higgs doublets vev's, one of the CP-even Higgs bosons acquires SM properties, while the second Higgs boson may be produced in association with the CP-odd Higgs boson state. In addition, the masses of the non-standard CP-even Higgs and the CP-odd Higgs are close to each other. Under these conditions, the mass bound on the SM-like CP-even Higgs is similar to the SM one, while the CP-odd and the second CP-even Higgs boson mass bound reads $m_h \gtrsim 90 \text{ GeV}$ [2].

In this paper, we will depart from these simple assumptions, by breaking the mass relations that appear in the simplest supersymmetric models, and studying the consequences of such modifications of the parameters of the theory. Indeed, while it has been a common belief that the Higgs boson will be eventually discovered at the upcoming LHC experiments, one would like to fully utilize the potential to search for the Higgs bosons at the Tevatron in these non-conventional scenarios as well. Non-standard mass relations are already present in extensions of the MSSM including an additional singlet (NMSSM [3, 4] and other extensions [5, 6, 7, 8, 9, 10]), or when explicit CP-violation exist in the Higgs sector [11]. In these cases, the SM-like Higgs (h) may dominantly decay into a pair of lighter Higgs (a), an admixture of CP even and odd states with a dominant CP odd component. (The precise fraction of the CP even or odd component is not crucial in the present study.) Therefore it is possible that the Higgs escaped detection at the LEP experiments by avoiding the usual decay modes such as $h \rightarrow b\bar{b}$, $\tau^+\tau^-$, WW^* and ZZ^* , and the lower limit on Higgs mass should be re-evaluated. The LEP collaborations have already analyze the possible constraints on Higgs boson production arising from this new decay mode [12, 13]. We shall use the results of these analyses as a starting point for our study. We are interested in analyzing the sensitivity of the Tevatron and the LHC experiments in the search for a light, SM-like Higgs boson with such an exotic decay mode.

We consider the case where the SM-like Higgs boson decays into a pair of spin-zero states, $h \rightarrow aa$, which in turn cascade into a heavy fermion pair $a \rightarrow b\bar{b}$ or $a \rightarrow \tau^+\tau^-$. These Higgs-to-Higgs decay modes have been studied extensively in NMSSM [14, 15, 16] at the LHC, together with even more complicated cascades. Most of these studies indeed take advantage of the dominant production modes of the Higgs boson at hadron colliders, i.e. gluon fusion and weak boson fusion, but encounter large SM backgrounds. We therefore consider the Higgs signal produced

in association with a W or Z boson, where the leptonic decays of the weak bosons will provide a clean trigger, and will significantly reduce the background as well.¹

The significance of associated production was also stressed in Ref. [19] for $h \rightarrow aa$ decays in NMSSM at the LHC. For similar parameter choices, our results lead to a comparable or slightly better reach for Higgs boson searches to the ones obtained in earlier studies [14, 15, 16] on gluon fusion and weak boson fusion productions at the LHC, while showing more discovery potential at the Tevatron than in previous studies.

2. Signal Processes and Parameter Choices

2.1 Signal Processes

For the two spin-zero states, a 's, the combinations of decay products we can search for are $4b$, $2b2\tau$ and 4τ . The 4τ mode is usually suppressed by the branching fractions, unless m_a is below the $b\bar{b}$ decay threshold [20]. We thus concentrate on the two channels $2b2\tau$ and $4b$ next. The signal events being searched are

$$Wh \rightarrow l\nu_l, aa \rightarrow \begin{cases} l\nu_l, b\bar{b}, b\bar{b} \\ l\nu_l, b\bar{b}, \tau^+\tau^- \end{cases} \quad (2.1)$$

$$Zh \rightarrow l^+l^-, aa \rightarrow \begin{cases} l^+l^-, b\bar{b}, b\bar{b} \\ l^+l^-, b\bar{b}, \tau^+\tau^-, \end{cases} \quad (2.2)$$

with $l = e, \mu$. The channel $Z \rightarrow \nu\nu$ decays into neutrino pairs can also be considered, while the triggering could be large missing energy, plus τ 's or b 's.

2.2 Parameter Choices

We would like to perform a relatively model-independent search for the signal, therefore the Higgs masses, branching fractions and couplings to the weak bosons are employed as input parameters. Direct searches for a Higgs boson with SM-like couplings to the gauge bosons, in a model and decay mode-independent way, leads to a lower bound on m_h of about 82 GeV [21] with full SM coupling to Z . On the other hand, the proposed search is expected to become inefficient for $m_h > 130$ GeV, since the standard decays into the WW^* and ZZ^* channels are still expected to be dominant. Therefore, the optimal setting to detect the Higgs decaying into an aa pair is to have the mass m_h within the range of 90 – 130 GeV. The choice for m_a can be more flexible. As long as $m_h > 2m_a$ and $m_a > 2m_b$ to kinematically allow the decays $h \rightarrow aa$ and $a \rightarrow b\bar{b}$, our methods are rather insensitive to the mass choices.

¹An initial analysis by us at the Tevatron was reported earlier in Ref. [17]. While this current work was in process, another similar analysis for the $4b$ channel at the LHC appeared [18]. For the overlap with that work at the LHC, our studies included more background analyses, more realistic b -tagging effects, and a broader parameter scan.

In a generic model, the Wh/Zh production rate differs from that in the SM. The change can be characterized by a prefactor κ_{hWW}^2 (κ_{hZZ}^2), where κ_{hVV} is the coupling strength of Higgs to vector boson V relative to that in the SM. The production cross section can thus be written in terms of the SM result with an overall factor to account for the modification of the coupling

$$\sigma(Vh) = \kappa_{hVV}^2 \sigma^{SM}(Vh). \quad (2.3)$$

We are interested in the range of $\kappa^2 \sim 0.5 - 1.0$, so that this Higgs contributes to the electroweak symmetry breaking and consequently the associated productions are still sizable.

In order for the $h \rightarrow aa$ decay to be dominant and thus escape the LEP bound, $BR(h \rightarrow aa)$ is required to be close to unity. For instance, in the NMSSM, $BR(h \rightarrow aa) > 0.9$ turns out to be very general in terms of the naturalness of c in the trilinear coupling term $(cv/2)haa$ [22]. Moreover, if the down quark and lepton coupling to the Higgs is proportional to their masses, then $BR(a \rightarrow b\bar{b})$ and $BR(a \rightarrow \tau^+\tau^-)$ are set to be 0.92 and 0.08, respectively. In general, however, the relations between the coupling and the masses may be modified by radiative corrections, which can lead to a large increase of the $BR(h \rightarrow \tau\tau)$ [23]. The representative values and the ranges of the parameters are summarized in Table 1, all allowed by constraints from LEP [12, 13], except for the region near $m_h \sim 90$ GeV when both a 's are assumed to decay into two bottom quarks. Parametric consistency with the LEP results is also discussed in detail [24] within the NMSSM framework.

	parameters	representative value	considered range
masses	m_h	120	90–130
	m_a	30	20–60
coupling	κ_{hVV}^2	0.7	0.5–1.0
branching fractions	$BR(h \rightarrow aa)$	0.85	0.8–1.0
	$BR(a \rightarrow b\bar{b})$	0.92	0.95–0.50
	$BR(a \rightarrow \tau^+\tau^-)$	0.08	0.05–0.50
$2b2\tau$ channel	$C_{2b2\tau}^2$	0.088	0.038–0.50
$4b$ channel	C_{4b}^2	0.50	0.10–0.90

Table 1: Parameter choices for $h \rightarrow aa$ decays. The C^2 factor is defined in the next section.

3. $h \rightarrow aa$ at the Tevatron

3.1 The $2b2\tau$ Channel

Including the decay branching fractions for $aa \rightarrow b\bar{b}\tau^+\tau^-$, we obtain the cross section

as

$$\sigma_{2b2\tau} = \sigma(Vh) BR(V) 2BR(h \rightarrow aa)BR(a \rightarrow b\bar{b})BR(a \rightarrow \tau^+\tau^-). \quad (3.1)$$

where $BR(V) = 0.213$ (0.067) is the leptonic branching fraction of W (Z) decay into $l = e, \mu$.

The overall factor modifying the SM result in Eq. (3.1),

$$C_{2b2\tau}^2 \equiv 2\kappa_{hVV}^2 BR(h \rightarrow aa)BR(a \rightarrow b\bar{b})BR(a \rightarrow \tau^+\tau^-), \quad (3.2)$$

corresponds to the process-dependent C^2 factor defined in the DELPHI search [12], and the S_{95} factor in the comprehensive LEP analysis [13]. Our parameter choice (range), as listed in Table 1, is equivalent to a $C_{2b2\tau}^2$ of 0.088 (0.038 – 0.50), consistent with the bounds for a large range of our m_h, m_a choices set forth in Refs. [12, 13]. A value of 0.088 for $C_{2b2\tau}^2$ is assumed for all numerical evaluations from here on, unless explicitly noted otherwise.

3.2 Signal Event Rate for the $2b2\tau$ Channel

The associated production of $p\bar{p} \rightarrow Wh$ usually features a larger cross section than that of Zh , and the leptonic branching fraction of W is about 3 times larger than Z 's. For illustration purposes, we choose to present our detailed studies for the Wh channel henceforth, although we will include the Zh channel in our results.

Total cross sections for $p\bar{p} \rightarrow Wh$ and $p\bar{p} \rightarrow Zh$ at hadron colliders have been calculated with QCD and electroweak corrections included [25, 26, 27] in the SM. Hence we get

$$\sigma^{SM}(Wh) BR(W \rightarrow l\nu_l) \sim 85 \text{ (24) fb} \quad (3.3)$$

at $\sqrt{s} = 1.96$ TeV for $m_h = 90$ (130) GeV.

Including the branching fractions and couplings, the cross section of the signal in Eq. (3.1) is

$$\sigma_{2b2\tau} \sim 7.5 \text{ (2.1) fb} \quad \text{for } C^2 = 0.088 \quad (3.4)$$

as illustrated in Fig. 1. The solid curve on top represents the total cross section for Vh production, with V decaying leptonically, but without any cuts. The dashed curve represents the cross section after adjusting for the couplings and branching fractions, as in Eq. (3.1). Cross sections for Zh are also plotted for completeness.

3.3 Background and Cuts for the $2b2\tau$ Channel

The main advantage for considering the process Wh is the possible background suppression due to the clean final state from the W leptonic decay: an isolated charged lepton ($l = e, \mu$) plus large missing transverse energy. We thus require the following initial acceptance cuts at the Tevatron [28]

$$p_T(l) > 15 \text{ GeV}, \quad |\eta(l)| < 2.0, \quad \cancel{E}_T > 15 \text{ GeV}. \quad (3.5)$$

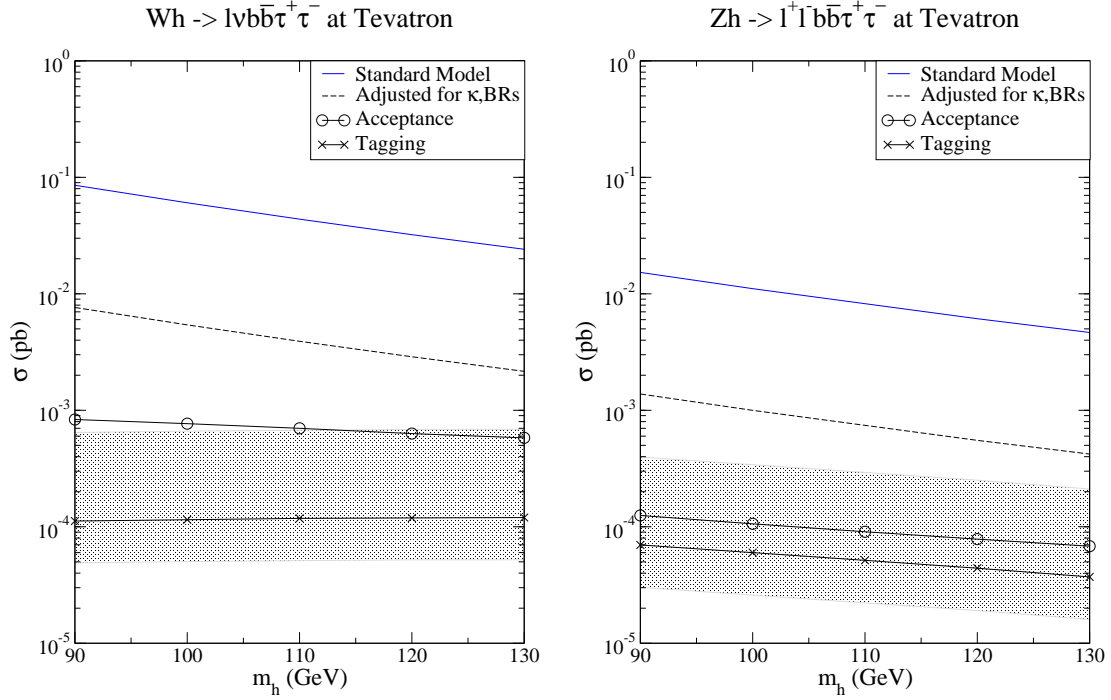


Figure 1: Cross sections of Higgs signal at the Tevatron in the $2b2\tau$ channel produced by Higgs-strahlung with a leptonically decaying W (left) or Z (right). The four lines from the top to the bottom correspond to, respectively, the SM cross section (solid line); adjusted for $C_{2b2\tau}^2 = 0.088$ and $m_a = 30$ GeV (dotted line); including the acceptance cuts Eqs. (3.5)–(3.8) (line with circles); and further including tagging efficiencies Eq. (3.9) (line with crosses). The shaded bands correspond to variations of the final results (line with crosses) for values of C^2 within the range considered in Table 1 and taking into account the LEP constraints [13].

The events have yet to further pass the acceptance cuts, or to have the taus and b 's tagged. Both help suppress the SM backgrounds, while bringing significant reductions to the event rate as well. Our challenges are to retain as many signal events as possible, and to control the backgrounds from various sources. Throughout the paper, we adopt the Monte Carlo program MadEvent [29] for our background simulations at the parton level.

b and τ Tagging We wish to identify events with 5 particles plus missing energy in the final states: $b\bar{b}\tau^+\tau^-l\nu_l$. With neutrinos in the decay products, tau momenta cannot be fully reconstructed. Therefore we cannot reconstruct the invariant masses $m(2\tau)$ or $m_h \sim m(2b2\tau)$. Instead, the signal should appear as a peak in the $m(2b)$ plot, around the value of m_a .

For the jets and other soft leptons in the events, the following basic cuts are

employed to mimic the CDF [30] detector acceptance, for jets [31]:

$$p_T(j) > 10 \text{ GeV}, \quad |\eta(j)| < 3.0, \quad (3.6)$$

and for τ -candidates [32]:

$$p_T > 10, 8, 5 \text{ GeV for } \tau_h, \tau_e, \tau_\mu, \quad |\eta| < 1.5. \quad (3.7)$$

where τ_e , τ_μ and τ_h stand for the visible decay products of $\tau \rightarrow e\nu_e\nu_\tau$, $\tau \rightarrow \mu\nu_\mu\nu_\tau$, and $\tau \rightarrow \text{hadrons} + \nu_\tau$, respectively, and an isolation cut

$$\Delta R > 0.4 \quad (3.8)$$

between leptons, τ 's and b -jets. After the acceptance cuts, 10 – 25% of the signal events survive, and the cross section becomes 0.85 (0.57) fb for $m_h = 90$ (130) GeV with the given set of input parameters ($C^2 \sim 0.088$). The cross sections passing acceptance are plotted in Fig. 1 versus the Higgs mass, represented by the circled curve. At this level, the cross section is below 1 fb.

The b - and hadronic τ -tagging efficiencies and the kinematics are taken to be

$$\begin{aligned} \epsilon_b &= 50\% \text{ for } E_T^{jet} > 15 \text{ GeV} \text{ and } |\eta_{jet}| < 1.0, \\ \epsilon_\tau &= 40\% \text{ for } E_{vis} > 20 \text{ GeV} \text{ and } |\eta| < 1.5. \end{aligned} \quad (3.9)$$

Outside these kinematical regions, the tagging efficiencies drop off sharply [33, 34]. We decide to tag one b and one tau. The energies for a jet and a lepton are smeared according a Gaussian distribution. The energy resolutions are taken to be

$$\frac{\Delta E_j}{E_j} = \frac{75\%}{\sqrt{E_j}} \oplus 5\%, \quad \frac{\Delta E_l}{E_l} = \frac{15\%}{\sqrt{E_l}} \oplus 1\%. \quad (3.10)$$

The missing energy is reconstructed according to the smeared observed particles. No further detector effects are included [35].

Irreducible Background The dominant source of the irreducible background, with the same final state as the signal,

$$W \ Z^*/\gamma^*(\rightarrow \tau^+\tau^-) \ b\bar{b}, \quad (3.11)$$

has the $b\bar{b}$ pair from a virtual gluon splitting, the $\tau^+\tau^-$ pair from an intermediate Z^*/γ^* and the charged lepton plus missing energy from a W boson. Our simulations show that the largest contribution come from events with the Z^* almost on-shell, while the $\tau^+\tau^-$ pair from a virtual photon can be more easily confused with the signal. After applying the acceptance cuts, the irreducible background is estimated to be around 0.01 fb, which is very small compared to the signal size. It is essentially absent given the luminosity expected at the Tevatron.

Reducible Background Reducible background arise from jets mis-identified as b 's, or as hadronically decaying taus. The mistag rate from a light quark is taken to be $0.5 - 1.0\%$ for tau and 0.5% for b , respectively [33, 34]. A charm quark has higher mistag probability to fake a b quark, that we take to be 10% [36]. In addition, the experiments cannot distinguish directly produced electrons (muons) from leptonically decaying taus. Thus the reducible backgrounds considered in our study are listed below.

- The background due to misidentified bottom comes from the process $2\tau 2j l + \cancel{E}_T$, which has a cross section of 5 fb. Considering the mistag rate and the additional cuts, it contributes 0.02 fb to the background events.
- The background due to misidentified τ differs for different decay modes of τ 's:
 - For $\tau_l \tau_h 2bl \cancel{E}_T$ ($2l2b\tau_h \cancel{E}_T$), it comes from $2\tau 2bj$ with \cancel{E}_T from the leptonic decays of both taus. The contribution is estimated at 0.003 fb.
 - For $\tau_h \tau_h 2bl \cancel{E}_T$, the background comes from $2j 2bl \cancel{E}_T$ and is estimated at 30 fb. It is then reduced by the tau-mistag rate, the b-tagging rate, and their associated cuts. In the continuum distribution of $m(2b)$, it is below the level of the resonant signal. Within the mass window of $10 \text{ GeV} < m(2b) < 70 \text{ GeV}$, this background accumulates to $0.04 - 0.09$ fb, depending on the τ mistag rate considered.
- The backgrounds from both a mistagged tau and a mistagged b mostly come from the $4jl \cancel{E}_T$ events, which has a cross section of about 16 pb. After the cuts and folding in the mistag rates, this contributes $0.03 - 0.05$ fb of background in $10 \text{ GeV} < m(2b) < 70 \text{ GeV}$, depending on the τ mistag rate considered.

The two bottom-quarks in the final state coming from the Higgs boson decays should have an invariant mass equal m_a . If enough data were available, one would be able to observe an excess of events in the $m(2b)$ mass distribution. However, this procedure is heavily limited by statistics. For instance, with a window cut of $m_a \pm 10 \text{ GeV}$ on $m(2b)$, the reducible background can be a factor of 3 to 5 smaller than the signal, but unfortunately, the cuts and the tagging efficiencies together reduce the signal greatly to about 0.11 fb for Wh and $0.05 - 0.07$ fb for Zh , with $C^2 \sim 0.088$ as shown in Fig. 1 by the crossed curve. The shaded band represents the range of parameters allowed by our choice of $C^2 \sim 0.038 - 0.50$, consistent with the LEP constraints. With an optimistic value of $C^2 \sim 0.50$, the cross section is 0.68 fb, and we would expect to see about a couple of signal events with an integrated luminosity of a few fb^{-1} .

To illustrate a most optimistic situation in terms of kinematical considerations, we explore the optimization between m_a and m_h to obtain the largest signal rate.

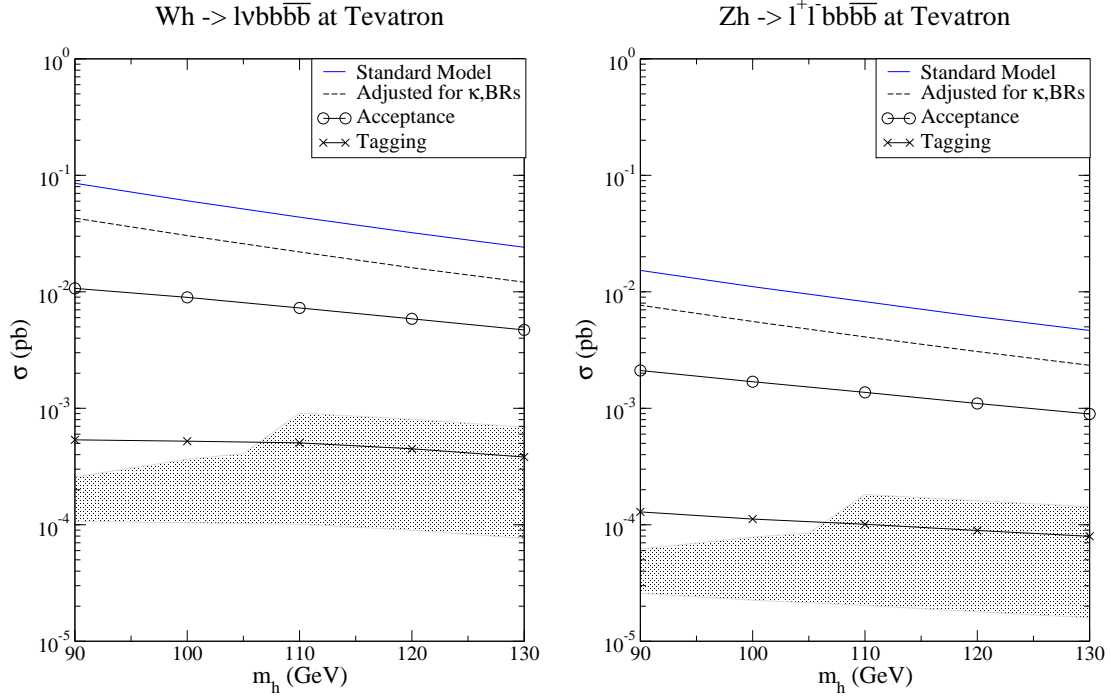


Figure 2: Cross sections of Higgs signal at the Tevatron in the $4b$ channel produced by Higgs-strahlung with a leptonically decaying W (left) or Z (right). The four curves from top to bottom correspond to, respectively, the SM cross section (solid line); adjusted for $C_{4b}^2 = 0.50$ and $m_a = 30$ GeV (dotted line); including the acceptance cuts Eqs. (3.5), (3.6) and (3.8) (line with circles); and further including tagging efficiencies Eq. (3.9) (line with crosses). The shaded bands correspond to variations of the final results (line with crosses) for values of C^2 within the range considered in Table 1 and taking into account the LEP constraints [13].

The signal loss is mainly due to the softness of the b and τ 's, therefore most events are rejected from the lower p_T threshold. Increasing m_a would stretch the p_T distributions to the higher p_T end. To achieve this without significantly affecting the decay phase space of h , we set

$$m_a = (m_h - 10 \text{ GeV})/2, \quad (3.12)$$

which resulted in more than doubling the signal rate with respect to the $m_a = 30$ GeV case as our default presentation throughout. In this case the signal cross section is ~ 0.28 fb for $C^2 = 0.088$, and ~ 1.6 fb for $C^2 = 0.50$, which is still challenging for observation with the Tevatron's projected luminosity.

3.4 The $4b$ Channel

As we mentioned earlier, the light spin-zero state a mostly decays into $b\bar{b}$ (50 – 95%) or $\tau^+\tau^-$ (5 – 50%). The $\tau^+\tau^-$ channel can be dominant when a is very light, *i.e.*

$m_a \lesssim 2m_b$. However it would be difficult to observe Higgs in the 4τ mode, first because of the increasing background near the lower end of $m(\tau\tau)$, and because of the difficulty in resolving highly-collimated tau pairs. These scenarios involving a very light a are among the difficult ones for NMSSM Higgs discovery discussed in Ref. [15]. A relevant 4τ study at the Tevatron under such scenario can be found in Ref. [20]. A very light a could also be probed through Upsilon or even J/Ψ decays [37]. For the $m_a > 2m_b$ case, we will next look for the Higgs in the $4b$ channel.

Similar to the $2b2\tau$ mode, the $4b$ cross section is

$$\sigma_{4b} = \sigma(Vh) BR(V) BR(h \rightarrow aa) BR(a \rightarrow b\bar{b})^2, \quad (3.13)$$

from which we extract the C^2 factor

$$C_{4b}^2 \equiv \kappa_{hVV}^2 BR(h \rightarrow aa) BR(a \rightarrow b\bar{b})^2. \quad (3.14)$$

The $4b$ mode is usually enhanced by the large branching fractions of the decay of a into bottom quarks. The ratio $C_{4b}^2/C_{2b2\tau}^2$ ranges in $9.5 - 0.5$ for $BR(a \rightarrow \tau\tau) \sim 0.05 - 0.50$. The value of C_{4b}^2 itself does not vary greatly with the branching fractions that are obtained within our choice of parameters, Table 1. Despite larger background for this mode than for the $2b2\tau$ mode, the enhanced rate suggests this to be a more viable mode.

The parameter choices for the $4b$ channel are also given in Table. 1. Running parallel to the $2b2\tau$ channel, we plot the cross sections in Fig. 2. The shaded bands show the LEP constraints disfavoring the lower end of the m_h range. We find the signal rate after acceptance cuts to be $10.7 - 4.7$ fb (the circled curve) for $m_h = 90 - 130$ GeV with $C^2 \sim 0.5$. After tagging three bottom jets (for reasons explained below) and imposing appropriate additional cuts, the cross section becomes $0.54 - 0.38$ fb (the crossed curve) for $m_h = 90 - 130$ GeV.

We again adopt the basic acceptance cuts and the b -tagging requirements as in the previous section. The background for this mode arises from $4bl\cancel{E}_T$, $3bjl\cancel{E}_T$, $2b2jl\cancel{E}_T$, $b3jl\cancel{E}_T$ and $4jl\cancel{E}_T$ events. For the four b 's in our signal, tagging two will not be sufficient, as background from $2b2jl\cancel{E}_T$ events can fake the signal without any mistagging involved. Therefore we demand that at least three bottom jets be tagged.

The irreducible background $4bl\cancel{E}_T$, though much larger than that in the $2b2\tau$ mode, is still manageable. We find the cross section to be 0.23 fb after basic acceptance cuts. Like the signal events, it suffers similar reductions from tagging and further cuts, which brings it down to 0.02 fb. With tagging for $3b$'s, the $3bjl\cancel{E}_T$ events cannot be effectively distinguished from the signal either. They contribute about 0.003 fb to the background.

The reducible backgrounds from $2b2jl\cancel{E}_T$ and $4jl\cancel{E}_T$ events have the same sources as that in the $2b2\tau$ mode and the mistag rates of a light jet to b and to τ are

comparable. The tagging on the 3rd b brings this background down significantly. In total, they contribute about 0.07 fb to the background. Another background source is from $2b2cl\cancel{E}_T$, which is approximately 2.5 times as large as that of $4bl\cancel{E}_T$ at the Tevatron. With a 10% mistag rate and after the acceptance cuts, it is reduced to 0.007 fb. Finally $3bjl\cancel{E}_T$ and $b3jl\cancel{E}_T$ backgrounds combine to contribute less than 0.003 fb.

Having tagged three of the four bottom quarks, we identify the fourth bottom as the hardest untagged jet in the event. We expect the signal to appear as a peak in the invariant mass $m(b_1, b_2)$ and $m(b_3, b_4)$ distribution. However, pairing the four b jets can be complicated due to combinatorics. We assign the two pairs by minimizing their mass difference $m(b_1, b_2) \approx m(b_3, b_4)$ and record both values each with a half weight. We present the signal versus the background distributions of the reconstructed masses m_h and m_a in Fig. 3 as the invariant masses of four b -jets and of two b -jets. With a simple cut on the $m(4b)$ invariant mass, $m(4b) < 160$ GeV, dictated by our search for a light Higgs boson with mass smaller than about 130 GeV, the overall signal to background ratio can be about 10 with $C^2 = 0.50$, $m_a = 30$ GeV and $m_h = 90 - 130$ GeV.

To summarize our study at the Tevatron, we claim that the signal channels of Eqs. (2.1) and (2.2) have distinctive kinematical features (see Fig. 3) with negligible SM backgrounds and the signal observation is total statistically dominated. For the $2b2\tau$ mode, one can reach a cross section of about 0.05–0.7 fb as shown in Fig. 1, while for the $4b$ mode, we have the cross section in the range of 0.1–1 fb as shown in Fig. 2. If the h and a masses happen to be related in an optimal way (Eq. (3.12)) we can gain an increase in the signal rate by a factor of ~ 1.8 and 2.5 for the $4b$ and $2b2\tau$ channels.

4. $h \rightarrow aa$ at the LHC

At the LHC, weak boson-associated Higgs production rate is about 10 – 15 times that at the Tevatron in the mass region we are interested in. With the same C^2 factor, signal events passing through acceptance also take on this ratio. The (QCD) background, on the other hand, can be 100 times larger than at the Tevatron. This requires a substantial jet rejection rate. These cross sections are plotted in Fig. 4.

Cuts on the triggering leptons and/or missing energy are taken to be

$$p_T(l) > 20 \text{ GeV}, \quad |\eta(l)| < 2.5, \quad \cancel{E}_T > 20 \text{ GeV}. \quad (4.1)$$

The following cuts and efficiencies for tagging are assumed [38]

$$\begin{aligned} \epsilon_b &= 50\% \text{ for } E_T^{jet} > 15 \text{ GeV} \text{ and } |\eta_{jet}| < 2.0, \\ \epsilon_\tau &= 40\% \text{ for } E_{vis} > 15 \text{ GeV} \text{ and } |\eta| < 2.5. \end{aligned} \quad (4.2)$$

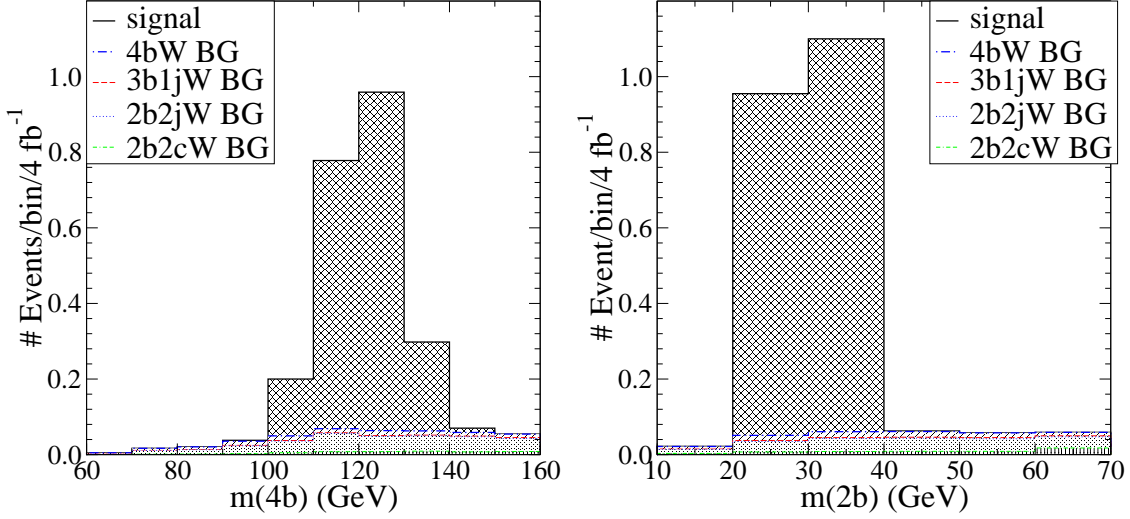


Figure 3: Higgs signal (double-hatched) on top of the sum of the backgrounds at the Tevatron in the $4b$ decay channel together with a leptonically decaying W . The invariant mass of four (left) and two (right) b -jets are shown. Values of $C_{4b}^2 = 0.50$, $m_h = 120$ GeV and $m_a = 30$ GeV are understood. From bottom to top, the background histograms indicate the accumulative sum of $2b2cW + 2b2jW + 3b1jW$ and $2b2cW + 2b2jW + 3b1jW + 4bW$.

The jet rejection rate is better than $1/150$ for tagging a b or a τ , except in the $15 - 30$ GeV p_T range where it is taken to be $\sim 1/30$, as there exists strong tension between tagging efficiencies and the jet rejection rates, especially near the low p_T range. Note that the jet rejection rate will only be accurately known after understanding the detectors with examining the real data. Again, in our simulations, the energies for a jet and a lepton are smeared with the Gaussian resolutions

$$\frac{\Delta E_j}{E_j} = \frac{50\%}{\sqrt{E_j}} \oplus 3\%, \quad \frac{\Delta E_l}{E_l} = \frac{10\%}{\sqrt{E_l}} \oplus 0.7\%. \quad (4.3)$$

The missing energy is reconstructed accordingly.

4.1 The $2b2\tau$ Channel

Similar to the Tevatron case, the irreducible background of Eq. (3.11) is small after the acceptance cuts and the tagging requirements, contributing only 0.07 fb. The reducible background, however, poses a much more severe problem at the LHC. For example, the $2b2j l \cancel{E}_T$ events are estimated to be around 11 pb, compared to 50 fb at the Tevatron. Thus for the $2b2\tau$ mode, a jet rejection rate of $1/150$ would give rise to a background of 92 fb, compared to the signal size of about 1 fb (or up to ~ 7 fb when maximizing C^2). The $4j l \cancel{E}_T$ events also contribute 43 fb to the background in this channel.

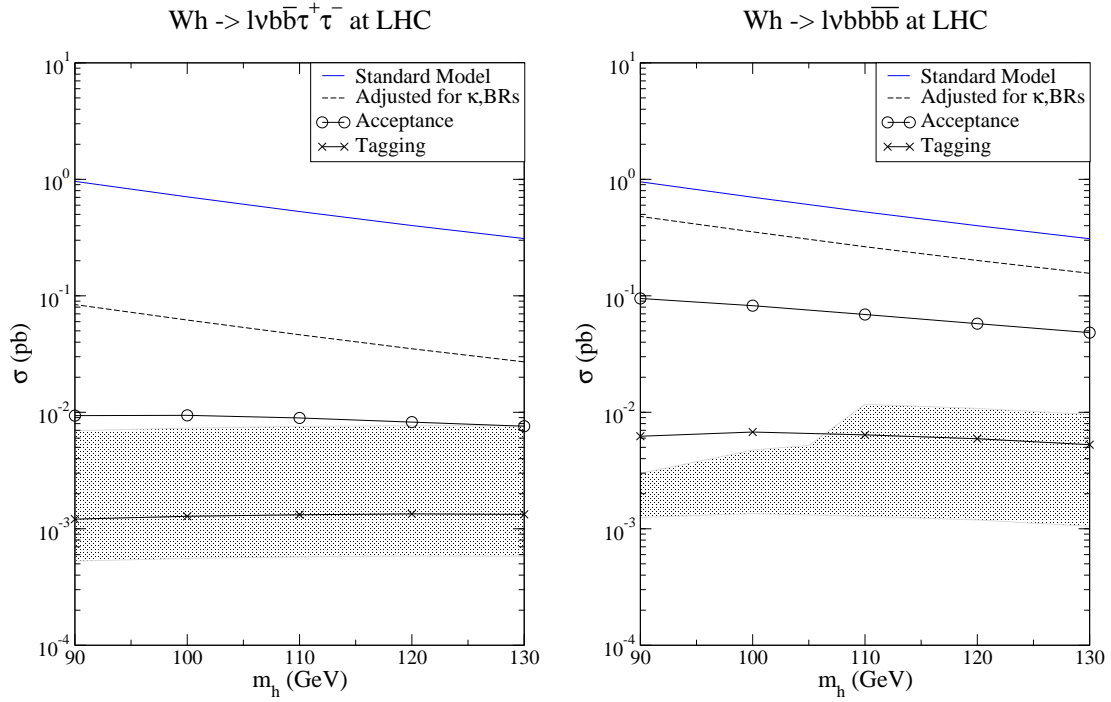


Figure 4: Cross sections of Higgs signal at the LHC in the $2b2\tau$ (left) and $4b$ (right) channels produced by Higgs-strahlung with a leptonically decaying W . The four curves from top to bottom correspond to, respectively, the SM cross section (solid line); adjusted for $C_{2b2\tau}^2 = 0.088$, $C_{4b}^2 = 0.50$ and $m_a = 30$ GeV (dotted line); including the acceptance cuts Eq. (4.1) (line with circles); and further including tagging efficiencies Eq. (4.2) (line with crosses). The shaded bands correspond to variations of the final results (line with crosses) for values of C^2 within the range considered in Table 1 and taking into account the LEP constraints [13].

We carry out the analysis similar to the Tevatron case and arrive at a S/B ratio of 0.03, with a total signal size of less than 1 fb for $m_h = 120$ GeV, $m_a = 30$ GeV and $C^2 = 0.088$. The small S/B ratio would require precise control of the systematic errors. It can be further improved by tagging one more b or τ , at the expense of losing up to half of the signal rate. Due to the difficulty of finding a signal in this channel, we are led to consider the more promising channel of $4b$'s, where, as we did in the Tevatron case, we employ an additional tagging, while still retaining a higher signal rate.

4.2 The $4b$ Channel

With a much higher luminosity than the Tevatron and larger cross sections, LHC could produce 60 (10 fb^{-1}) to over a thousand (300 fb^{-1}) Higgs events in the $4b l \cancel{E}_T$ decay channel, assuming a typical C^2 value ($C_{4b}^2 = 0.50$), as shown in Fig. 4. The

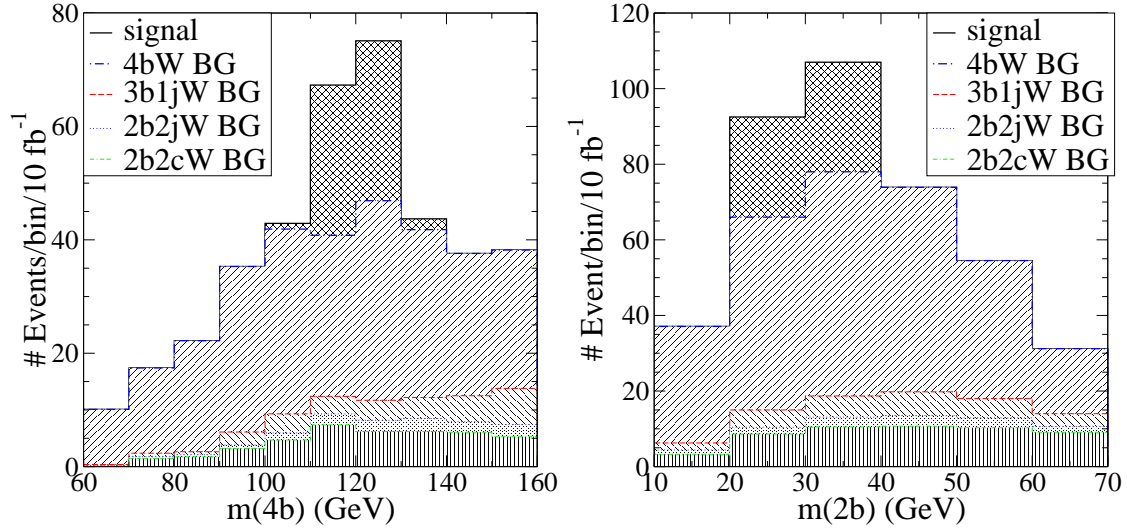


Figure 5: Higgs signal (double-hatched) on top of the sum of the backgrounds at the LHC in the $4b$ decay channel together with a leptonically decaying W . The invariant mass of four (left) and two (right) b -jets are shown. Constraints of $60 \text{ GeV} < m(4b) < 160 \text{ GeV}$ and $10 \text{ GeV} < m(2b) < 70 \text{ GeV}$ are implemented in both plots. $C_{4b}^2 = 0.50$, $m_h = 120 \text{ GeV}$ and $m_a = 30 \text{ GeV}$ are understood. From bottom to top, the background histograms indicate the accumulative sum of $2b2cW$, $2b2cW + 2b2jW$, $2b2cW + 2b2jW + 3b1jW$, and $2b2cW + 2b2jW + 3b1jW + 4bW$, respectively.

$4b$ channel is thus more optimistic for observing the Higgs, even though the background still dominates the signal, and the irreducible $4bl\cancel{E}_T$ background becomes non-negligible. We require tagging three of the b jets, which would essentially eliminates backgrounds from $4jl\cancel{E}_T$, and reduces the $2b2jl\cancel{E}_T$ and $1b3jl\cancel{E}_T$ background significantly. With three tagged b -jets, the signal rate is about 5.7 fb (or up to 10 fb when maximizing C^2). The irreducible background $4bl\cancel{E}_T$ is 25 fb. The $3bjl\cancel{E}_T$ background is about 16 fb. The reducible background from $2b2jl\cancel{E}_T$ events is about 80 fb, and $2b2cl\cancel{E}_T$ is about 4 fb with a 10% mistag rate for $c \rightarrow b$ [38]. The $4jl\cancel{E}_T$ background is no larger than 0.2 fb.

We again present the reconstructed mass distribution for the signal and backgrounds in two plots in Fig. 5. The left and right plots show the invariant mass distributions of the $4b$ and $2b$ system, where the signal peaks near $m_h = 120 \text{ GeV}$ and $m_a = 30 \text{ GeV}$, respectively, each with a width less than 10 GeV due to detector energy resolution. Similar to the Tevatron case, we assign the two bb pairs by minimizing their mass difference $m(b_1, b_2) \approx m(b_3, b_4)$ and plot these two masses, each with a half weight.

The dominant $2b2jl\cancel{E}_T$ background comes from $t\bar{t}$ production. For $t\bar{t}$ events, the $2b2j$ system contains all the decay products of a top-quark. Therefore, these events

may be efficiently rejected with an upper cut on the $m(4b)$ invariant mass lower than the top quark mass, $m(4b) \lesssim 160$ GeV, which will not affect the signal we consider if the Higgs boson mass is in the region $m \lesssim 130$ GeV. Given our considered range of choices, we implement the following constraints in the two distributions:

$$\begin{aligned} 10 \text{ GeV} &< m(2b) < 70 \text{ GeV} , \\ 60 \text{ GeV} &< m(4b) < 160 \text{ GeV} . \end{aligned}$$

While the former affects the $m(4b)$ distribution minimally, the latter reduces the background in $m(2b)$ distribution by about 40%.

Overall, selecting events with these invariant mass constraints, the value of S/B is roughly $1/5$ for $C_{4b}^2 = 0.50$. Assuming a good understanding of the background, one can get an estimate of the statistical significance of the signal. For the rate quoted above we obtain a significance, S/\sqrt{B} , of over 3.5σ for 10 fb^{-1} and over 5σ for 30 fb^{-1} , as indicated in Fig. 5. If one selects events only in the expected signal region, we obtain a $S/B \simeq 0.41$ in the range $100 \text{ GeV} < m(4b) < 140 \text{ GeV}$ from the $m(4b)$ distribution, and a $S/B \simeq 0.40$ in the range $20 \text{ GeV} < m(2b) < 40 \text{ GeV}$ from the $m(2b)$ distribution, equivalent to a reduction by about a factor of two of the luminosity necessary to achieve the same statistical significances. The challenge is for us to understand the background well enough, and to control the systematic errors.

It may be a challenge at the LHC to retain the high b -tagging efficiency at $p_T \sim 15 \text{ GeV}$ adopted in the current analysis. If a 30 GeV cut on the tagged jets is implemented instead, the signal is reduced to 22%, while the background drops to about 37% of the values given above. In such case a 3σ (5σ) signal would require an integrated luminosity of around 30 (80) fb^{-1} . Therefore a good understanding of b -tagging efficiencies at low p_T will be necessary to be able to discover a Higgs in the $4b$ channels in the first years of the LHC.

Before closing this section, a remark is in order for comparing our results with a recent similar analysis for the $4b$ channel at the LHC [18]. Their conclusions are somewhat more optimistic, largely due to a significantly higher b -tagging efficiency assumed (70%). They did not consider the QCD backgrounds of $W2b2c$ and $W2b2j$, which are sub-leading. On the other hand, we neglected the background $t\bar{t}b\bar{b}$ considered in [18] since with the additional energetic W from the top-quark decay $E_W \approx \frac{m_t}{2} \sqrt{1 - M_W^2/m_t^2}$, this background can be efficiently removed by vetoing the extra jet or charged lepton activities from the W decay.

5. Summary

The search for a Higgs boson with couplings to the gauge bosons of the order of the SM one, and decaying into two lighter CP-odd Higgs bosons states may be performed

at hadron colliders for the associate production of Wh , Zh with $h \rightarrow aa$ ($2b2\tau$ or $4b$). The cross sections scale proportionally to C^2 , a factor determined by the product of the relevant branching fractions times the ratio of the Higgs production cross section to the SM one. Maximal event rates of the two channels are given by different values of $BR(a \rightarrow \tau\tau)$. SM-like $af\bar{f}$ couplings tend to give small $BR(a \rightarrow \tau\tau)$, thus suppressing the $2b2\tau$ channel and enhancing the $4b$ channel. In models where $BR(a \rightarrow \tau\tau)$ is large, the $2b2\tau$ channel yields an event rate comparable to the $4b$ channel.

We analyzed the Wh channel in the mass range $90 \leq m_h \leq 130$ GeV in detail. We found that at the Tevatron

- With only basic cuts, the signal size is 0.7 fb for the $2b2\tau$ channel for $C_{2b2\tau}^2 \sim 0.088$ with a negligible irreducible background, and 5 – 10 fb for the $4b$ channel for $C_{4b}^2 \sim 0.50$ with a comparable background. With favorable couplings and branching fractions, the C^2 factor can be as large as 0.50 for the $2b2\tau$ mode, and 0.90 for the $4b$ mode, and the signal rate is enhanced proportionally.
- Further cuts and the tagging of b and τ , necessary to remove the much larger reducible background, worsen the signal event rate to around 0.11 fb for the $2b2\tau$ mode and 0.5 fb for the $4b$ mode, as summarized in Figs. 1 and 2. However, the kinematics of the mass reconstruction of m_a and m_h can be very distinctive, as seen in Fig. 3 for the $4b$ mode with small background and a couple of total events.
- We also consider the most favorable relations between m_h and the CP-odd Higgs mass m_a , which can enhance the signal rate by a factor of 2.5 for the $2b2\tau$ mode leading to a cross section as large as 1.6 fb with $C_{2b2\tau}^2 = 0.5$, and by a factor of 1.8 for the $4b$ mode leading to a value 1.8 fb for $C_{4b}^2 = 0.9$.
- There can be another improvement of 15 – 30% by combining Wh events with the Zh events, where both $Z \rightarrow ll$ and $Z \rightarrow \nu\nu$ can be included, leading to a possible observation of a few events in either $2b2\tau$ or $4b$ channel, for a Tevatron luminosity of the order of a few fb^{-1} .

Overall, the signal observation becomes statistically limited. Our study has been based on parameters of the CDF detector. One expects the signal observability to be enhanced accordingly if results from the D0 detector were combined.

At the LHC, the signal rate increases by a factor of 10, and the background increases by two orders of magnitude, compared to the Tevatron. We found that

- Statistics limitation is no longer a major issue. In the $4b$ channel alone the signal rate is 5.7 fb, and we can easily obtain a signal significance S/\sqrt{B} greater than 3.5 with an integrated luminosity of 10 fb^{-1} , and over 10 with 100 fb^{-1} .

- Similar to the Tevatron study, with favorable couplings and branching fractions, the signal rate can be enhanced to be as large as 10 fb with $C^2 = 0.9$, as seen in Fig. 4, and S/B can be improved accordingly.
- The kinematics of the mass reconstruction of m_a and m_h can be very distinctive, as seen in Fig. 5 for the $4b$ mode, yielding a statistically significant signal.
- Favorable m_h and m_a relations, combinations of the Wh and Zh signals, combinations of the $2b2\tau$ channel with the $4b$ channel, could all improve the signal rate and enhance the potential to the eventual discovery of the Higgs boson.

The main challenge would be to retain the adequate tagging efficiency of b 's and τ 's in the low p_T region.

We point out that our background analysis is based on the leading order partonic calculations in MadEvent. More accurate estimate of the background distributions would be important to claim a signal observation. More realistic simulations including the detector effects are needed to draw more convincing conclusions.

Acknowledgments

TH and G.-Y.H were supported in part by a DOE grant No. DE-FG02-95ER40896 and in part by the Wisconsin Alumni Research Foundation. Work at ANL is supported in part by the US DOE, Div. of HEP, Contract DE-AC02-06CH11357. Fermilab is operated by Universities Research Association Inc. under contract no. DE-AC02-76CH02000 with the DOE.

References

- [1] **LEP Working Group for Higgs boson searches** Collaboration, R. Barate *et al.*, *Search for the standard model Higgs boson at LEP*, *Phys. Lett.* **B565** (2003) 61–75, [[hep-ex/0306033](#)].
- [2] **ALEPH** Collaboration, A. Heister *et al.*, *Final results of the searches for neutral Higgs bosons in $e^+ e^-$ collisions at \sqrt{s} up to 209-GeV*, *Phys. Lett.* **B526** (2002) 191, [[hep-ex/0201014](#)].
- [3] R. Dermisek and J. F. Gunion, *Escaping the large fine tuning and little hierarchy problems in the next to minimal supersymmetric model and h to $a a$ decays*, *Phys. Rev. Lett.* **95** (2005) 041801, [[hep-ph/0502105](#)].
- [4] T. Han, P. Langacker, and B. McElrath, *The Higgs sector in a $U(1)'$ extension of the MSSM*, *Phys. Rev.* **D70** (2004) 115006, [[hep-ph/0405244](#)].

- [5] M. Cvetič, D. A. Demir, J. R. Espinosa, L. L. Everett, and P. Langacker, *Electroweak breaking and the μ problem in supergravity models with an additional $U(1)$* , *Phys. Rev.* **D56** (1997) 2861–2885, [[hep-ph/9703317](#)].
- [6] C. Panagiotakopoulos and K. Tamvakis, *New minimal extension of MSSM*, *Phys. Lett.* **B469** (1999) 145–148, [[hep-ph/9908351](#)].
- [7] C. Panagiotakopoulos and A. Pilaftsis, *Higgs scalars in the minimal non-minimal supersymmetric standard model*, *Phys. Rev.* **D63** (2001) 055003, [[hep-ph/0008268](#)].
- [8] B. A. Dobrescu and K. T. Matchev, *Light axion within the next-to-minimal supersymmetric standard model*, *JHEP* **09** (2000) 031, [[hep-ph/0008192](#)].
- [9] J. Erler, P. Langacker, and T.-J. Li, *The $Z - Z'$ mass hierarchy in a supersymmetric model with a secluded $U(1)'$ -breaking sector*, *Phys. Rev.* **D66** (2002) 015002, [[hep-ph/0205001](#)].
- [10] V. Barger, P. Langacker, and G. Shaughnessy, *Singlet extensions of the MSSM*, *AIP Conf. Proc.* **903** (2007) 32–39, [[hep-ph/0611112](#)].
- [11] M. Carena, J. R. Ellis, S. Mrenna, A. Pilaftsis, and C. E. M. Wagner, *Collider probes of the MSSM Higgs sector with explicit CP violation*, *Nucl. Phys.* **B659** (2003) 145, [[hep-ph/0211467](#)].
- [12] **DELPHI** Collaboration, J. Abdallah *et al.*, *Searches for neutral Higgs bosons in extended models*, *Eur. Phys. J.* **C38** (2004) 1, [[hep-ex/0410017](#)].
- [13] **ALEPH** Collaboration, S. Schael *et al.*, *Search for neutral MSSM Higgs bosons at LEP*, *Eur. Phys. J.* **C47** (2006) 547–587, [[hep-ex/0602042](#)].
- [14] U. Ellwanger, J. F. Gunion, C. Hugonie, and S. Moretti, *Towards a no-lose theorem for NMSSM Higgs discovery at the LHC*, [hep-ph/0305109](#).
- [15] U. Ellwanger, J. F. Gunion, and C. Hugonie, *Difficult scenarios for NMSSM Higgs discovery at the LHC*, *JHEP* **07** (2005) 041, [[hep-ph/0503203](#)].
- [16] S. Chang, P. J. Fox, and N. Weiner, *Naturalness and Higgs decays in the MSSM with a singlet*, *JHEP* **08** (2006) 068, [[hep-ph/0511250](#)].
- [17] U. Aglietti *et al.*, *Tevatron-for-lhc report: Higgs*, [hep-ph/0612172](#).
- [18] K. Cheung, J. Song, and Q.-S. Yan, *Role of $h \rightarrow \eta\eta$ in intermediate-mass higgs boson searches at the large hadron collider*, *Phys. Rev. Lett.* **99** (2007) 031801, [[hep-ph/0703149](#)].
- [19] S. Moretti, S. Munir, and P. Poulose, *Another step towards a no-lose theorem for NMSSM Higgs discovery at the LHC*, *Phys. Lett.* **B644** (2007) 241, [[hep-ph/0608233](#)].

- [20] P. W. Graham, A. Pierce, and J. G. Wacker, *Four taus at the Tevatron*, [hep-ph/0605162](#).
- [21] **OPAL** Collaboration, G. Abbiendi *et al.*, *Decay-mode independent searches for new scalar bosons with the OPAL detector at LEP*, *Eur. Phys. J. C* **27** (2003) 311–329, [[hep-ex/0206022](#)].
- [22] B. A. Dobrescu, G. Landsberg, and K. T. Matchev, *Higgs boson decays to CP-odd scalars at the Tevatron and beyond*, *Phys. Rev. D* **63** (2001) 075003, [[hep-ph/0005308](#)].
- [23] M. Carena, S. Mrenna, and C. E. M. Wagner, *MSSM Higgs boson phenomenology at the Tevatron collider*, *Phys. Rev. D* **60** (1999) 075010, [[hep-ph/9808312](#)].
- [24] R. Dermisek and J. F. Gunion, *Consistency of LEP event excesses with an h to a decay scenario and low-fine-tuning NMSSM models*, *Phys. Rev. D* **73** (2006) 111701, [[hep-ph/0510322](#)].
- [25] T. Han and S. Willenbrock, *QCD correction to the $p p \rightarrow W H$ and $Z H$ total cross-sections*, *Phys. Lett. B* **273** (1991) 167–172.
- [26] M. L. Ciccolini, S. Dittmaier, and M. Kramer, *Electroweak radiative corrections to associated $W H$ and $Z H$ production at hadron colliders*, *Phys. Rev. D* **68** (2003) 073003, [[hep-ph/0306234](#)].
- [27] T. Hahn, S. Heinemeyer, F. Maltoni, G. Weiglein, and S. Willenbrock, *SM and MSSM Higgs boson production cross sections at the Tevatron and the LHC*, [hep-ph/0607308](#).
- [28] **D0** Collaboration, V. M. Abazov *et al.*, *Search for associated Higgs boson production $WH \rightarrow WWW^* \rightarrow \ell^\pm \nu \ell'^\pm \nu' + X$ in $p\bar{p}$ collisions at $\sqrt{s} = 1.96$ TeV*, *Phys. Rev. Lett.* **97** (2006) 151804, [[hep-ex/0607032](#)].
- [29] F. Maltoni and T. Stelzer, *MadEvent: Automatic event generation with MadGraph*, *JHEP* **02** (2003) 027, [[hep-ph/0208156](#)].
- [30] **CDF IIb** Collaboration, P. T. Lukens, *The CDF IIb detector: Technical design report*, . FERMILAB-TM-2198.
- [31] **CDF** Collaboration, T. Aaltonen *et al.*, *First measurement of the production of a W boson in association with a single charm quark in proton anti-proton collisions at $\sqrt{s}=1.96$ TeV*, *Phys. Rev. Lett.* **100** (2008) 091803, [[arXiv:0711.2901](#) [[hep-ex](#)]].
- [32] **CDF** Collaboration, *Search for neutral MSSM Higgs bosons decaying to tau pairs in $p\bar{p}$ collisions at $\sqrt{s} = 1.96$ TeV*, *Phys. Rev. Lett.* **96** (2006) 011802, [[hep-ex/0508051](#)].
- [33] **CDF** Collaboration, D. Acosta *et al.*, *Search for new physics using high mass tau pairs from 1.96- TeV p anti- p collisions*, *Phys. Rev. Lett.* **95** (2005) 131801, [[hep-ex/0506034](#)].

- [34] **CDF** Collaboration, D. Jeans, *B tagging at CDF*, . Presented at Hadron Collider Physics Symposium 2005, Les Diablerets, Switzerland.
- [35] **CDF** Collaboration, A. Abulencia *et al.*, *Measurements of inclusive W and Z cross sections in $p\bar{p}$ collisions at $\sqrt{s} = 1.96$ TeV*, *J. Phys.* **G34** (2007) 2457, [[hep-ex/0508029](#)].
- [36] **CDF** Collaboration, D. Acosta *et al.*, *Measurement of the $t\bar{t}$ production cross section in $p\bar{p}$ collisions at $\sqrt{s} = 1.96$ TeV using lepton + jets events with secondary vertex b -tagging*, *Phys. Rev.* **D71** (2005) 052003, [[hep-ex/0410041](#)].
- [37] R. Dermisek, J. F. Gunion, and B. McElrath, *Probing NMSSM scenarios with minimal fine-tuning by searching for decays of the Upsilon to a light CP-odd Higgs boson*, *Phys. Rev.* **D76** (2007) 051105, [[hep-ph/0612031](#)].
- [38] **ATLAS** Collaboration, *ATLAS: Detector and physics performance technical design report. volume 1*, . CERN-LHCC-99-14.